HHS Public Access

Author manuscript

Sci Transl Med. Author manuscript; available in PMC 2018 December 06.

Published in final edited form as:

Sci Transl Med. 2017 December 06; 9(419): . doi:10.1126/scitranslmed.aal2332.

Bexarotene-activated PPARδ promotes neuroprotection by restoring bioenergetic and quality control homeostasis

Audrey S. Dickey[1], **Dafne N. Sanchez**[1], **Martin Arreola**[1], **Kunal R. Sampat**[1], **Weiwei Fan**[2], **Nicolas Arbez**[3], **Sergey Akimov**[3], **Michael J. Van Kanegan**[4], **Kohta Ohnishi**[1], **Stephen K. Gilmore-Hall**[1], **April L. Flores**[1], **Janice M. Nguyen**[1], **Nicole Lomas**[1], **Cynthia L. Hsu**[1], **Donald C. Lo**[4], **Christopher A. Ross**[3,5], **Eliezer Masliah**[6,7], **Ronald M. Evans**[2,8], and **Albert R. La Spada**[1,7,9,10,11,12]

[1]Department of Pediatrics, University of California, San Diego; La Jolla, CA 92093, USA

[2]Gene Expression Laboratory, Salk Institute for Biological Studies, San Diego, CA 92037, USA

[3]Department of Psychiatry, Johns Hopkins University School of Medicine, Baltimore, MD 21287, USA

[4]Center for Drug Discovery and Department of Neurobiology, Duke University Medical Center, Durham, NC 27710, USA

[5]Department of Neurology, Pharmacology, and Neuroscience, Johns Hopkins University School of Medicine, Baltimore, MD 21287, USA

[6]Department of Pathology, University of California, San Diego; La Jolla, CA 92093, USA

[7]Department of Neurosciences, University of California, San Diego; La Jolla, CA 92093, USA

[8]Howard Hughes Medical Institute, Salk Institute for Biological Studies, San Diego, CA 92037, USA

[9]Department of Cellular & Molecular Medicine, University of California, San Diego; La Jolla, CA 92093, USA

[10]Division of Biological Sciences, University of California, San Diego; La Jolla, CA 92093, USA

[11]Institute for Genomic Medicine, University of California, San Diego; La Jolla, CA 92093, USA

[12]Sanford Consortium for Regenerative Medicine, University of California, San Diego; La Jolla, CA 92093, USA

Corresponding author: Albert La Spada, MD, PhD, Cellular & Molecular Medicine, Neurosciences, and Pediatrics, University of California, San Diego, 2880 Torrey Pines Scenic Drive, MC 0642, La Jolla, CA 92037-0642, (858)-246-0148 [ph.], alaspada@ucsd.edu.

Author contributions: A.S.D. and A.R.L.S provided the conceptual framework for the study. A.S.D. and A.R.L.S. designed all the experiments, with assistance from W.F. and R.M.E. for extracellular flux analysis, D.C.L. for the cortico-striatal neuron co-culture experiments, C.A.R. for the human stem cell-derived neuron studies, and E.M. for EM48 immunohistochemistry and neuropathology analysis. A.S.D., D.N.S., M.A., K.R.S., N.A., S.A., M.J.V.K., K.O., S.K.G.-H., A.L.F., J.M.N., N.L., C.L.H., and D.C.L. performed the experiments. A.S.D. and A.R.L.S. wrote the manuscript.

Competing interests: The authors have no competing interests to declare, no consulting relationships to declare, and no relevant patents pending on this work.

Data Availability: All data needed to evaluate the conclusions in the study are present in the paper and the Supplementary Materials. Receipt of human HD stem cell materials requires completion of a MTA.

Abstract

Neurons must maintain protein and mitochondrial quality control for optimal function, an energetically expensive process. The PPARs are ligand-activated transcription factors that promote mitochondrial biogenesis and oxidative metabolism. We recently determined that transcriptional dysregulation of PPARδ contributes to Huntington's disease (HD), a progressive neurodegenerative disorder resulting from a CAG-polyglutamine repeat expansion in the huntingtin gene. We documented that the PPARδ agonist KD3010 is an effective therapy for HD in a mouse model. PPARδ forms a heterodimer with the retinoid X receptor (RXR), and RXR agonists are capable of promoting PPARδ activation. One compound with potent RXR agonist activity is the FDA-approved drug bexarotene. Here, we tested the therapeutic potential of bexarotene in HD, and found that bexarotene was neuroprotective in cellular models of HD, including medium spiny-like neurons generated from induced pluripotent stem cells (iPSCs) derived from patients with HD. To evaluate bexarotene as a treatment for HD, we treated the N171-82Q mouse model with the drug and found that bexarotene improved motor function, reduced neurodegeneration, and increased survival. To determine the basis for PPARδ neuroprotection, we evaluated metabolic function and noted markedly impaired oxidative metabolism in HD neurons, which was rescued by bexarotene or KD3010. We examined mitochondrial and protein quality control in cellular models of HD, and observed that treatment with a PPARδ agonist promoted cellular quality control. By boosting cellular activities that are dysfunctional in HD, PPARδ activation may have therapeutic applications in HD and potentially other related neurodegenerative diseases.

Introduction

Huntington's disease (HD) is a progressive autosomal dominant neurodegenerative disorder in which patients develop motor and cognitive impairment (1). HD pathology is defined by degeneration and death of medium spiny neurons (MSNs) of the striatum, as well as cortical pyramidal neurons that project to the striatum (2, 3). In 1993, a CAG trinucleotide repeat expansion mutation in the coding region of the huntingtin (htt) gene was identified as the cause of HD (4). As observed in other polyglutamine (polyQ) repeat diseases, htt glutamine tracts that exceed a certain length threshold (~37 repeats in HD) adopt a new pathogenic confirmation and are resistant to the normal processes of protein turnover, leading to cellular toxicity and neurodegeneration (5). The length of the mutant htt polyQ expansion inversely correlates with the age of disease onset and rate of disease progression in HD patients.

Neurons in the brain require continued production of high-energy compounds by mitochondria. We, and others, have linked mitochondrial dysfunction in HD to transcription dysregulation of peroxisome proliferator-activated receptor gamma coactivator-1 alpha (PGC-1α), a co-activator that coordinates transcriptional programs that culminate in mitochondrial biogenesis and enhanced oxidative metabolism (6–8). The importance of PGC-1α for HD pathogenesis is underscored by the observation that PGC-1α overexpression is sufficient to rescue motor dysfunction, prevent accumulation of misfolded htt protein, and stave off neurodegeneration in HD mice (9). To determine the mechanistic basis for PGC-1α transcription interference in HD, we performed an unbiased screen that showed PPARs to be htt interactors, and documented an interaction between PPARδ and htt

in non-neuronal cells, in striatal-like neurons, and in the cerebral cortex of HD mice (10). We noted that PPARδ is highly expressed in neurons of the central nervous system (CNS), and demonstrated that expression of dominant-negative PPARδ in CNS is sufficient to produce motor phenotypes, neurodegeneration, mitochondrial defects, and transcriptional abnormalities that closely parallel HD disease phenotypes (10). We then evaluated a selective, potent PPARδ agonist, KD3010, and after confirming that it crosses the blood brain barrier to up-regulate expression of PPARδ target genes in cortex and striatum, we tested KD3010 in N171-82Q transgenic mice, a rodent model of HD. This study established the efficacy of KD3010 PPARδ agonist therapy as a potential therapeutic approach for HD (10).

One facet of PPARδ biology with relevance to therapy development is that PPARδ forms a heterodimer with RXR, and the resulting “permissive” PPARδ - RXR heterodimer is subject to dual ligand regulation, meaning that RXR agonists can promote PPARδ activation (11). One drug compound with potent RXR agonist activity is bexarotene, a synthetic product structurally similar to retinoic acid compounds, known endogenous RXR ligands. Bexarotene (targretin) is FDA-approved for use in patients with T-cell cutaneous lymphoma. One provocative study reported that bexarotene administration to a mouse model of Alzheimer’s disease (AD) yielded a dramatic rescue of cognitive, social, and olfactory deficits, accompanied by improved neural circuit function and enhanced clearance of soluble Aβ oligomers (12). The mechanistic basis for this effect was proposed to involve increased PPARγ activation (13). As PPARδ is highly expressed in CNS neurons, more so than PPARγ (14), the mechanistic basis for the therapeutic action of bexarotene in AD deserves reconsideration, in light of our discovery of a role for PPARδ in maintaining normal nervous system function (10), and recent work demonstrating the neuroprotective effect of PPARδ agonist treatment in AD mice (15).

Here, we considered the neurotherapeutic potential of bexarotene in HD, and found that bexarotene was neuroprotective in multiple cellular models of HD, ranging from mouse striatal and cortical neurons to medium spiny neurons generated from induced pluripotent stem cells (iPSCs) derived from patients with HD. We then treated the N171-82Q HD mouse model with bexarotene and observed improved neuron survival and motor function. To determine the molecular basis for PPARδ agonist therapy, we evaluated metabolic dysfunction in HD, and documented markedly impaired oxidative metabolism in HD neurons, which was rescued by bexarotene or KD3010. We examined mitochondrial and protein quality control in cellular models of HD, and observed that PPARδ agonist therapy achieved neuroprotection by promoting quality control function.

Results

Bexarotene promotes PPARδ activation to achieve neuroprotection

To evaluate the effect of bexarotene on PPARδ activation, we co-transfected PPARδ and a 3x-PPAR response element (3x-PPRE) luciferase reporter construct into primary cortical neurons derived from a bacterial artificial chromosome transgenic HD mouse model (BAC-HD) containing the full-length huntingtin gene with 97 glutamine repeats or into primary cortical neurons derived from littermate control (WT) mice, and noted marked induction of

PPARδ activation upon bexarotene treatment (Fig. 1A). Bexarotene promotion of PPARδ activation was comparable to PPARδ activation using a PPARδ-selective agonist GW501516 (Fig. 1A). We also observed a marked increase in PPARδ activation when we boosted RXR expression (Fig. S1A), corroborating the permissive nature of PPARδ activation upon heterodimerization with RXR (11). To determine if bexarotene-induced PPARδ activation countered mutant huntingtin (htt) neurotoxicity, we assessed the effect of bexarotene treatment on mitochondrial dysfunction and cell death in BAC-HD neurons. When we measured mitochondrial membrane potential using two different fluorescent probes, we noted significantly reduced mitochondrial membrane potential in BAC-HD neurons, which was rescued upon bexarotene treatment (Fig. 1B and Fig. S1B). Similarly, bexarotene treatment yielded a significant reduction in the frequency of BAC-HD neurons that displayed caspase-3 activation, an indicator of impending cellular demise (Fig. 1C). Previous studies of bexarotene neuroprotection in an AD mouse model have proposed that bexarotene neuroprotection relies upon activation of PPARγ (12). To determine the basis for bexarotene neuroprotection in HD neurons, we repeated bexarotene treatment of BAC-HD primary neurons along with concurrent knockdown of either PPARα, PPARδ, or PPARγ, which was accomplished by co-expression of shRNA vectors directed against each of the different PPARs (Fig. S1C). When we measured mitochondrial membrane potential in BAC-HD neurons treated with bexarotene and subjected to knock-down of either PPARα, PPARδ, or PPARγ, we found that bexarotene rescue of mitochondrial membrane potential occurred despite PPARα or PPARγ knock-down, but was prevented by concurrent knock-down of PPARδ (Fig. 1D). Bexarotene neuroprotection was not limited to BAC-HD primary cortical neurons, as bexarotene treatment also improved mitochondrial function and cell survival of WT neurons; enhanced WT neuron function upon exposure to bexarotene also depended upon PPARδ (Fig. S1D–E). We then assayed bexarotene rescue of BAC-HD neuron cell death, and noted that PPARδ knock-down eliminated any benefit from bexarotene treatment, while PPARα or PPARγ knock-down did not significantly affect bexarotene neuroprotection (Fig. 1E). Finally, to determine if bexarotene treatment of BAC-HD primary neurons promoted increased PPARδ activation, we measured the RNA expression of PPARδ targets previously shown to respond to PPARδ agonist treatment pharmacodynamically in mice (10). We documented bexarotene-induced expression of these PPARδ target genes (Fig. 1F). We noted that combined bexarotene + GW501516 treatment often yielded even greater increases in PPARδ target gene expression (Fig. 1F).

To further evaluate bexarotene neuroprotection in HD, we pursued experiments in different models of mutant htt neurotoxicity that aim to recapitulate HD neuropathology. First, we transfected co-cultured mouse cortical neurons and striatal neurons with N-terminal htt containing 90 amino acids with either an 8-glutamine repeat (Nt-90-8Q) or a 73-glutamine repeat expansion (Nt-90-73Q), and treated co-cultured cortical-striatal neurons with increasing bexarotene concentrations. We observed a significant increase ($P < .05$ or $P < .01$) in neuron survival in a dose-dependent manner (Fig. 2A–B). We then tested the effect of bexarotene in primary cortical neurons transfected with N-terminal htt containing 586 amino acids with an 82-glutamine repeat expansion (Nt-586-82Q), and noted a dose-dependent reduction ($P < .01$ or $P < .001$) in neuron cell death (Fig. 2C). We also differentiated human HD induced pluripotent stem cells into striatal medium spiny-like neurons, and transferred

them to brain-derived neurotrophic factor (BDNF)-free Neural Induction Medium (NIM), as withdrawal of neurotrophic factor support promotes neuron cell death. To evaluate rescue, we supplemented the media with either bexarotene or brain-derived neurotrophic factor (BDNF), which robustly prevented neuron cell death in this system. We observed marked protection of HD medium spiny-like neurons from cell death upon either bexarotene or BDNF treatment (Fig. 2D). These findings indicate that bexarotene can ameliorate mutant htt neurotoxicity.

Bexarotene treatment improves motor function and rescues neurodegeneration in HD mice

As bexarotene displayed neuroprotection against mutant htt toxicity, and is already approved for use in humans, we pursued a therapy trial of bexarotene in N171-82Q mice, which recapitulate HD-like motor phenotypes and neurodegeneration within a time frame of 5 – 6 months (16). Bexarotene is a lipophilic molecule that readily crosses the blood brain barrier in rodents (17, 18). To establish the dosage for a preclinical trial, we performed a pharmacodynamics study by delivering bexarotene via intraperitoneal (i.p.) injection, at either 10 mg/kg or 30 mg/kg for 3 days /week for one week, to 6 week-old WT C57BL/6J mice, and then measuring PPARδ target gene expression in the striatum. We observed comparable increases in PPARδ target gene expression in the brains of mice on the 10 mg/kg dosage regimen and the 30 mg/kg dosage regimen (Fig. S2). However, we noted that the 30 mg/kg bexarotene dosage regimen was not well tolerated, causing significant morbidity. The 10 mg/kg bexarotene dosage regimen did not cause weight loss or visible side effects, based upon a neurological screening exam, nor did we detect any evidence of organ toxicity at necropsy.

Next, we injected N171-82Q mice with either 10 mg/kg /day of bexarotene or vehicle, 3 times per week, beginning at 6 weeks of age. Importantly, we adhered to recommended preclinical trial guidelines, intended to avoid spurious results (19, 20). We tracked the progression of disease phenotypes in vehicle-treated and bexarotene-treated HD mice by performing a composite neurological examination (21) and rotarod analysis at monthly intervals. Bexarotene treatment rescued neurological dysfunction and improved motor function in HD mice, as compared to vehicle-treated HD mice (Fig. 3A–B, Fig. S3A–D). Bexarotene also extended lifespan in HD mice by an average of 9.8 days (Fig. 3C). Neuropathology analysis further indicated that bexarotene treatment yielded a reduction in htt protein aggregates and prevented neuron cell loss in the striatum of HD mice (Fig. 3D–F).

Bexarotene rescues PPARδ target gene expression in both CNS and skeletal muscle of HD mice

To confirm that bexarotene treatment elicited induction of PPARδ activation in HD mice, we measured the expression of the PPARδ target genes angiopoietin-like 4 (*Angplt4*) and uncoupling protein 2 (*Ucp2*) in the cortex and striatum of bexarotene-treated mice, and documented marked increases in *Angplt4* and *Ucp2* expression in comparison to vehicle-treated HD mice (Fig. 4A–B). In human patients, sampling of CNS tissues was not feasible. As PPARδ is highly expressed in skeletal muscle, a practical alternative strategy would be to measure PPARδ target gene expression in this highly accessible tissue in the HD mice. We

thus assayed the expression of five PPARδ target genes, uncoupling protein 2 (*Ucp2*), adipose differentiation-related protein (*Adfp)*, lipoprotein lipase (*Lpl*), pyruvate dehydrogenase kinase isoform 4 (*PDK4*), and stearoyl-CoA desaturase 1 (*Scd1*), in quadriceps muscle samples obtained from WT controls, bexarotene-treated HD mice, and vehicle-treated HD mice. For all tested PPARδ target genes except *Lpl*, we observed rescue of gene expression; for *Pdk4* and *Scd1*, we noted dramatic up-regulation of expression at 3 to 5-fold that of WT HD mice (Fig. 4C). To assess the rapidity of productive PPARδ target engagement in mouse skeletal muscle, we assembled two additional cohorts of HD N171-82Q mice, and we treated one HD cohort with vehicle, and the other HD cohort with bexarotene at 10 mg/kg for one week. Significant induction of PPARδ target gene expression in quadriceps muscle was detected for three of the five targets in HD mice treated with bexarotene for just one week (Figure S4). These results indicate that PPARδ target gene expression in mouse skeletal muscle could serve as a marker of response to PPARδ agonist treatment.

PPARδ agonist treatment restores oxidative metabolic function in HD mice

Our bexarotene preclinical trial in HD mice, together with a recent preclinical trial of the PPARδ agonist KD3010 (10), suggest that PPARδ agonists may be a potential treatment for HD. How does PPARδ agonist treatment achieve *in vivo* neuroprotection? PPARδ has been shown to improve bioenergetics function by promoting mitochondrial ATP generation in skeletal muscle (22, 23). Mitochondrial dysfunction is a key feature of HD pathogenesis (24). To determine if PPARδ agonist treatment affected mitochondrial function in HD, we performed a bioenergetics profile of HD mouse primary cortical neurons in comparison to WT mouse primary cortical neurons, and evaluated the effects of bexarotene and KD3010. Extracellular flux analysis revealed that HD mouse neurons displayed a markedly reduced oxygen consumption rate (OCR) at baseline compared to WT neurons, and that the spare respiratory capacity of HD neurons, reflected by the maximal OCR, was also markedly reduced in comparison to WT neurons (Fig. 5A). As PPARγ was shown to drive ATP generation through mitochondrial oxidation of fatty acids (25), we supplied WT and HD mouse primary cortical neurons with palmitate, but this substrate did not produce any further differences in oxidative metabolism between WT and HD neurons. Treatment with bexarotene or KD3010 yielded a dramatic improvement in both basal OCR and maximal OCR in HD neurons (Fig. 5A–C), restoring OCR to that of WT neurons. In addition to measuring OCR, we also recorded rates of glycolysis by assaying the extracellular acidification rate, and confirmed that HD neurons produce ATP primarily via glycolysis, but that bexarotene or KD3010 treatment reverts HD neurons to an oxidative mode of energy production (Fig. 5D). Given the potency of PPARδ agonist treatment for boosting oxidative metabolism in HD neurons, we measured the effect of bexarotene or KD3010 treatment on WT neurons, and noted significant increases in basal OCR ($P < .01$) and maximal OCR ($P < .05$) (Fig. S5A), indicating that PPARδ activation is also capable of boosting bioenergetics function in WT neurons. To determine the relevance of this bioenergetics profile of HD primary neurons to the effects of bexarotene treatment *in vivo*, we performed qRT-PCR analysis on striatal RNAs for subsets of PPARδ target genes whose protein products function in the oxidative phosphorylation, glycolysis, or gluconeogenesis pathways. We documented restoration of a gene expression pattern matching the WT oxidative profile for bexarotene-

treated mice (Fig. 5E). When we extended this analysis to skeletal muscle from bexarotene-treated and KD3010-treated HD mice, we observed a similar phenomenon (Fig. S5B).

PPARδ improves mitochondrial and protein quality control to achieve neuroprotection

Neurons are placed under a constant demand for energy, and are in a continual battle to maintain mitochondrial quality control and protein quality control. Decompensation of proteostasis and mitochondrial quality control are defining features of neurodegenerative diseases, including HD (24, 26). As quality control processes are extremely energy intensive, and PGC-1α genetic rescue prevents protein aggregation and boosts mitochondrial function (9), we reasoned that PPARδ agonist treatment may ameliorate defects in mitochondrial quality control and protein quality control through its rescue of metabolic function. To test this hypothesis, we examined the mitochondrial morphology of striatal-like neurons carrying homozygous CAG-111 repeat expansion mutations in the mouse huntingtin (*Hdh*) gene (ST-*Hdh* Q111/Q111) (27). Comparison of ST-*Hdh* Q111/Q111 cells with control ST-*Hdh* Q7/Q7 cells revealed an increase in mitochondrial fragmentation in Q111/Q111 cells (Fig. 6A–B). Bexarotene treatment of ST-*Hdh* Q111/Q111 striatal-like cells yielded a significant reduction ($P < .05$ or $P < .01$) in mitochondrial fragmentation in a dose-dependent fashion (Fig. 6B). As PPARδ agonist treatment boosted metabolic function in normal neurons (Fig. S4A), we tested the effect of PPARδ activation on ST-*Hdh* Q7/Q7 cells, and observed an increase in mitochondrial length; we detected a reduction in mitochondrial length upon PPARδ knock-down (Fig. 6C). Oxidative stress impairs mitochondrial quality control, promoting fragmentation (28). When we treated ST-*Hdh* Q7/Q7 striatal-like cells with hydrogen peroxide, we observed a marked reduction in mitochondrial length, and this mitochondrial length reduction could be ameliorated by combined PPARδ over-expression and bexarotene treatment (Fig. 6D). Similarly, hydrogen peroxide yielded markedly greater mitochondrial fragmentation in ST-*Hdh* Q111/Q111 striatal-like cells, which was rescued by combined PPARδ over-expression and bexarotene agonist treatment (Fig. 6E). To assess the *in vivo* relevance of these findings, we quantified mitochondrial genomic DNA (mitoDNA) and nuclear genomic DNA (nDNA) in the striatum of bexarotene-treated HD mice. We documented a significant increase in the mitoDNA : nDNA ratio, which is an index of the abundance of mitochondrial biomass, in HD mice treated with bexarotene (Fig. 6F).

To determine if PPARδ activation status affects protein quality control, we employed a Neuro2a cell culture model of mutant htt aggregation, where transfection of N-terminal htt protein with 104 glutamine repeats yields marked aggregate formation in Neuro2a cells subjected to oxidative stress (9). Using this system, we found that treatment with the PPARδ agonist GW501516 or bexarotene elicited a marked reduction in htt-Q104 protein aggregation (Fig. 7A), and confirmed that bexarotene-mediated turnover of mutant htt protein was RXR dependent (Fig. S6). To establish which arm of the proteostasis pathway was responsible for the bexarotene-mediated reduction in htt aggregation, we performed htt-104Q transfection of Neuro2a cells in the presence of bexarotene, in combination with either lactacystin or spautin-1. We found that spautin-1 inhibition of autophagy blunted the reduction of htt aggregation achieved with bexarotene treatment (Fig. 7B). Knock-down of the autophagy-related 7 gene *(Atg7)* similarly yielded a significant blunting of bexarotene-mediated htt aggregate rescue in this system (Fig. 7B). To directly evaluate the effect of

PPARδ activation on autophagy, we assayed autophagy flux in Neuro2a cells subjected to PPARδ shRNA knock-down or PPARδ agonist activation, and noted a significant reduction in autophagy flux upon PPARδ knock-down, and a significant increase in autophagy flux with PPARδ agonist activation (Fig. 7C). This increase in autophagy flux could also be achieved with bexarotene activation of RXR (Fig. 7D). Transcription factor EB (TFEB) is a master regulator of autophagy (29), and upon PGC-1α induction, TFEB expression increases, thereby promoting autophagy (9). To assess the role of TFEB in PPARδ activation of autophagy, we measured autophagy flux in HeLa cells deficient in TFEB (Fig. S7A–B). We detected an increase in autophagy flux upon PPARδ agonist treatment that was comparable to the increased autophagy flux observed in WT HeLa cells treated with a PPARδ agonist (Fig. S7C–D), thereby ruling out a role for TFEB in PPARδ-mediated autophagy activation. To determine if bexarotene amelioration of mutant htt protein aggregation depended upon PPARδ activation, we quantified htt-Q104 aggregation in Neuro2a cells treated with bexarotene in the presence or absence of a specific PPARδ inhibitor (GSK3787), and noted that PPARδ inhibition abrogated bexarotene amelioration of htt protein aggregation (Fig 7E). These findings indicate that PPARδ activation achieves neuroprotection by improving mitochondrial and protein quality control pathways.

Discussion

HD and other neurodegenerative disorders, including AD and Parkinson's disease (PD), share two key defining cellular pathologies: mitochondrial dysfunction and impaired protein-organelle quality control. We, and others, previously linked mitochondrial dysfunction and transcription dysregulation in HD to interference with the transcription co-activator PGC-1α (6, 8, 30). As mutant htt does not directly interact with PGC-1α to blunt its function, we pursued the mechanistic basis for this transcription interference, and identified the nuclear hormone receptor PPARδf as a direct target of mutant htt neurotoxicity (10). As PPARδ heterodimerizes with RXR to activate its target genes, and the resulting "permissive" PPARδ-RXR heterodimer is subject to dual ligand regulation, RXR agonists are capable of promoting PPARδ activation (11). Here, we examined bexarotene in various *in vitro* cellular models of HD, and observed robust neuroprotection, suggesting the neurotherapeutic potential of bexarotene in HD. We pursued a therapy trial of bexarotene in HD N171-82Q mice, and using a study design that adhered to guidelines for rigor and reproducibility (19, 20), we documented improvements in motor function, htt protein aggregation, striatal neurodegeneration, and mouse survival.

Bexarotene (also called targretin) is approved for use in humans for T-cell cutaneous lymphoma, but is also currently in clinical trials in AD patients, based upon prior preclinical trial work in an AD mouse model (12). The mechanistic basis for the therapeutic efficacy of bexarotene was proposed to be increased activation of PPARγ, supporting a presumed role for enhanced Aβ clearance by PPARγ-expressing microglia (13). As PPARδ is highly expressed in CNS neurons (14), and bexarotene can also potently activate PPARδ, we sought the basis for bexarotene-mediated neuroprotection in BAC-HD primary neurons by concurrently knocking down the expression of PPARα, PPARδ, or PPARγ. For all tested readouts, we found that PPARδ is required for amelioration of mutant htt neurotoxicity. Our findings thus suggested that bexarotene neuroprotection involved PPARδ activation, and that

enhanced PPARδ activation could be contributing to the beneficial effects of bexarotene in AD (12, 31). Interestingly, whereas bexarotene readily crosses the blood brain barrier in rodents (17, 18), it does not efficiently cross the blood brain barrier in healthy human subjects (32), implying that bexarotene therapeutic responses observed in neurodegenerative disease patients may stem from the peripheral benefits of RXR and PPARδ activation, or from alteration of blood brain barrier function in human patients (33).

An important question that we sought to answer in this investigation was how PPARδ achieved neuroprotection. Numerous studies have examined the role of PPARδ in skeletal muscle, and these efforts led to the realization that PPARδ strongly favors oxidative metabolism, resulting in an increase in ATP (22, 23). Indeed, increased PPARδ activation in skeletal muscle is sufficient to yield profound changes in muscle physiology and endurance exercise performance. These changes have been linked to altered gene expression that enhances the function of the tricarboxylic acid (TCA) cycle and oxidative phosphorylation pathway (22, 23), preservation of glucose concentrations (34), and boosting of PGC-1α (35). We recently surveyed the expression of the PPARs, and found that only PPARδ is highly expressed in CNS neurons (10). We further found that transgenic expression of a dominant-negative PPARδ mutant in mice resulted in marked neurodegeneration in the context of diminished electron transport chain activity and greatly reduced ATP (10). We therefore directly assayed metabolic function by performing extracellular flux analysis on cortical neurons from BAC-HD mice, and observed marked reductions in OCR. These metabolic defects were reversed when we treated HD neurons with bexarotene or the PPARδ agonist KD3010, indicating that PPARδ agonist therapy, whether achieved with a PPARδ agonist or RXR agonist, is capable of reverting HD neurons from glycolytic metabolism to oxidative metabolism.

Neurons are unique as they are post-mitotic, have high energy requirements, and are exquisitely vulnerable to misfolded protein stress and defects in organelle quality control. Misfolded proteins, or peptide fragments thereof, are a defining feature of neurodegenerative disorders, including HD, PD, and AD (36). Neurons thus require energy not only for synaptic neurotransmission and transport of materials back and forth along their dendrites and axons, but also to maintain protein and organelle quality control. We reasoned that impaired oxidative metabolism in HD likely deprives neurons of the energy required to maintain mitochondrial quality control and proteostasis, especially given that altered mitochondrial dynamics and proteostasis are well established characteristics of HD pathology. Indeed, evidence from patient material, cell culture models, and BAC-HD mice indicates that HD neurons contain highly fragmented mitochondria (37–39). As excessive mitochondrial fission occurs in HD, likely due to altered regulation of the fission regulatory proteins Drp1 and Fis1 (38, 40, 41), dysregulation of mitochondrial dynamics in HD implies that maintenance of normal mitochondrial morphology in HD requires an even greater expenditure of energy. Support for this view comes from ultrastructural analysis of mice that recapitulate HD phenotypes upon expressing dominant-negative PPARδ in striatal neurons, whose mitochondria appear highly fragmented (10). After confirming that excessive mitochondrial fragmentation occurs in ST-*Hdh* Q111/Q111 mouse striatal-like cells, we treated Q111/Q111 cells with bexarotene and observed reductions in mitochondrial fragmentation. We further found that improved energy production can counter mitochondrial

fragmentation induced by oxidative stress in normal striatal-like cells, suggesting that PPARδ activation may be capable of supporting mitochondrial quality control in different stress situations.

In our bexarotene HD mouse study and in a previous study of PGC-1α over-expression (9), these interventions yielded reductions in htt protein aggregation in the brains of HD mice. To determine how bexarotene activation of PPARδ promotes proteostasis, we tested the effect of proteasome inhibition or autophagy inhibition on the bexarotene-mediated reduction of htt aggregates, and found that autophagy inhibition sharply countered htt aggregate reduction in bexarotene-treated cells. We documented markedly increased autophagy flux when we transfected cells with PPARδ in the presence of an agonist, but noted diminished autophagy flux when we performed PPARδ knock-down. Hence, our results indicate that PPARδ activation can upregulate autophagy, in agreement with prior work where PPARδ agonist treatment of cardiomyocytes yielded increased LC3-II, suggestive of autophagy induction; analysis of PPARδf knock-out mice revealed reductions in autophagy markers in the heart (42). As PGC-1α can promote increased expression of TFEB (9), a master regulator of autophagy, we evaluated the effect of PPARδ modulation in TFEB knock-out cells and observed that PPARδ activation yielded increased autophagy flux in the absence of TFEB, indicating that PPARδ upregulation of autophagy is not TFEB dependent.

A frequent observation in neurodegenerative diseases is the failure of mitochondrial energy production to keep up with CNS demand for ATP, coupled with an inability to maintain protein quality control and organellular homeostasis. Importantly, energy production and quality control function are inextricably linked, as neurons require energy for proteostasis and organelle quality control, and protein and organelle quality control must operate efficiently if a neuron is to retain a complement of fully functional mitochondria to carry out the task of ATP generation. If one arm of this homeostasis loop is disrupted, the other arm of the loop will inevitably become dysfunctional, and worsening dyshomeostasis will ensue, as the altered process will act as a positive feedback loop. In HD, we and others have discovered a central role for impaired mitochondrial energy production and quality control (6, 9, 30), and we have homed in on PPARδ as a regulatory factor capable of promoting oxidative metabolism to yield energy. As energy is necessary for promoting mitochondrial quality control at the level of mitochondrial dynamics, we tested if PPARδ activation could rescue mitochondrial fragmentation in HD, and found that PPARδ activation prevented mitochondrial fragmentation in HD cells. In HD, as in other neurodegenerative diseases, there is selective vulnerability of certain types of neurons. In the case of HD, it is striatal medium spiny neurons that are preferentially lost. Although the basis for this selective vulnerability is unknown, certain studies have found that striatal neurons are prone to mitochondrial fragmentation, due to increased expression of the Drp1 receptor Fis1 (43), a pro-fission effect of dopaminergic signaling (40), or increased S-nitrosylation of Drp-1 (41). Thus, in HD, the energy demands of medium spiny neurons, together with a predisposition to fragmentation of the mitochondrial network, may explain why PPARδ transcription interference contributes to HD pathogenesis, and why PPARδ promotion of mitochondrial fusion in HD is neuroprotective.

In this study, we considered an alternate approach for PPARδ activation, based upon its formation of permissive heterodimers with RXR, and found that bexarotene treatment counters mutant htt toxicity both *in vitro* and *in vivo* in HD. Our findings thus indicate that bexarotene deserves consideration as a potential therapy for HD; however, as this study only evaluated bexarotene in a HD mouse model featuring expression of truncated protein, further study of bexarotene in a HD mouse model featuring expression of full-length huntingtin protein is warranted. Furthermore, while HD mouse models recapitulate many aspects of the human disease, their predictive value for gauging the potential utility of a therapeutic intervention remains uncertain. Performing parallel studies in cell culture, mouse primary neurons, and human stem cell models is necessary to corroborate evidence for an agent's neuroprotection, and although this strategy was employed here, it is important to recognize that these systems also have their limitations. Although bexarotene is approved for use in humans, its use is associated with side effects that can be dose limiting (44). We have previously shown that the PPARδ agonist KD3010 is capable of robust neuroprotection in HD (10). Whereas KD3010 was found to be safe in humans in a Phase 1b clinical trial, its dosage range for chronic, long-term use has yet to be established. Because bexarotene and KD3010 act on different transcription factors, one appealing approach would be to employ combinatorial therapy in which the dosages of each compound could be reduced to limit their respective side effects, while achieving an additive or perhaps even synergistic treatment response in HD patients.

Materials & Methods

Study design

The primary objective of this study was to determine if the RXR agonist bexarotene was an effective treatment for HD. Bexarotene was evaluated in primary mouse neurons and human patient stem cell-derived neurons in experiments that used quantitative real-time PCR and assays of mitochondrial function and cell death. Bexarotene was tested in a preclinical trial in a mouse model of HD, with motor function, neuropathology, and survival as the outcome measures. The preclinical trial, which was approved by and performed in accordance with the UCSD Institutional Animal Care and Use Committee, adhered to a protocol where we arbitrarily divided littermates and balanced genders between experimental groups, with behavioral testing performed by investigators blinded to the treatment group of the mice. We based our group sizes upon power analysis to achieve 80% likelihood of detection of a 30% rescue of motor phenotypes. In the second half of this study, we sought the mechanisms by which PPARδ agonists achieved neuroprotection in our HD mouse model using experiments that employed quantitative real-time PCR, in vitro assays, immunohistochemistry, and Western blotting. For all experiments, replicate numbers are stated in the Figure legends.

Cell culture and primary neuron studies

ST-*Hdh* cells were cultured as previously (45). Primary cortical neurons from BAC-HD and wildtype mice were prepared as previously (10, 46). Co-transfection with indicated constructs (previously described (10)) was done with Lipofectamine 3000 as per manufacturer's protocol (Invitrogen). Lentiviral transduction was used to induce gene expression or knockdown in primary neurons, with infection achieved by adding 1×10^7

titer units of lentivirus to the culture media. For reporter assays, cells were drug-treated 24 hrs after reporter transfection, harvested 24 hrs later, and subjected to analysis using the Dual-Luciferase® Reporter Assay system (Promega). Mitochondrial membrane potential was measured via live cell loading with a potential-sensitive dye, either JC-1 or TMRM, using the Tecan M200Pro Reader. JC-1 was used for preliminary tests, followed up by more extensive mitochondrial characterization by Seahorse metabolism analysis. Analysis of cell death with immunofluorescence to activated caspase-3 was performed as described (47). H_2O_2 treatment was 25 μM for 4 hrs. Glucose starvation was done for 2 hrs in DMEM without glucose and 10% dialyzed FBS. Treatments with PPARδ antagonist GSK3787 (GSK), Lactacystin (L6785, Sigma-Aldrich), spautin-1 (SML0440, Sigma-Aldrich), and Bafilomycin A1 (B1793, Sigma-Aldrich) were as indicated for individual experiments. In all experiments, the investigator was blinded to culture conditions and cell treatments.

Primary mouse cortical neurons were prepared from CD1 mice as described previously (48). Co-transfection was performed at DIV5 with the N586 fragment of Huntingtin containing either 22Q (N586-Htt 22Q) or 82Q (N586-Htt 82Q) and eGFP (10:1 ratio) with lipofectamine 2000 according to the manufacturer's protocol. 1 μM Bexarotene treatment was done at the time of transfection. After 48 hrs of expression, cells were fixed with 4% paraformaldehyde for 30 min and nuclei were stained with Hoechst 33258 (bis-benzimide, Sigma-Aldrich). Image acquisition was done using the Axiovision imaging software on an Axiovert 100 inverted microscope (Carl Zeiss). Analysis and quantification were performed using Volocity (Perkin-Elmer). Nuclear staining intensity of GFP positive cells was measured, and neurons with a nuclear intensity of up to 200% of the intensity of healthy control were considered viable.

Primary rat cortical and striatal neurons were isolated from E18 Sprague-Dawley rat brains as described previously (49). Briefly, Nt-90-8Q and Nt-90-73Q constructs were transfected into separately isolated cortical and striatal neurons using electroporation. Cortical and striatal neurons were also co-transfected with YFP or mCherry respectively, as separate viability markers, then co-cultured on previously established glial cell beds for 5 days, prior to automated counting of YFP or mCherry neurons (49). Total numbers counted for fluorescently transfected neurons for each condition were normalized to Htt Nt-90-8Q-transfected neurons at baseline, with survival arbitrarily set to 1.

Animal studies and preclinical trial

All animal experimentation adhered to NIH guidelines and was approved by and performed in accordance with the UCSD IACUC. Cohort sizes were designated based upon power analysis for threshold effects of at least 25% difference. After genotyping, we performed motor baseline assessment prior to group assignments, and divided littermates and balanced genders between experimental groups, in accordance with guidelines intended to avoid spurious results (19, 20). After group assignment, we initiated Mon-Wed-Fri intraperitoneal injections of 10mg/kg/day bexarotene as a suspension in corn oil (3 mg/mL) at 6 weeks of age. Blinded observers visually inspected mice for obvious neurological signs and examined mice with a composite neurological evaluation tool, as previously (50), and also examined motor phenotypes, by performing rotarod testing as previously (10). For neuropathology

experiments, brains were harvested and histopathology, volume measurements, and stereology analysis were performed as previously (10). In all cases, the scorer was blinded to the genotype status and treatment condition of the mice.

Real-time RT-PCR analysis

RNA samples were isolated using Trizol (Life Technologies). Genomic DNA was removed using RNAse free DNAse (Ambion). mRNA quantification was performed using the 7500 Real Time PCR System (ABI) with ABI Assays-on-Demand primers and TaqMan® based probes (51) or using the SYBR green system (52). ABI TaqMan primer and probe set designations are available upon request. 18S or b-actin RNA were used as internal controls. Relative expression levels were calculated via the δδCt method.

Western blot analysis

Proteins were run on 10% Bis-Tris gels (Invitrogen) and transferred to PVDF membranes (Millipore) prior to blocking in Odyssey Blocking Buffer (LI-COR biosciences). Membranes were incubated with antibodies as indicated: LC3 (NB100-2220, Fisher), from Cell Signaling: TFEB (4240S), p-S6K (9234), p-S6 (2215) or β-actin (ab8226, Abcam), and imaged on the Odyssey (Licor).

Mitochondrial studies

The OCR and ECAR of primary neurons grown in Seahorse plates were measured using an extracellular Flux Analyzer (Seahorse Bioscience), following the manufacturer's instructions. The Seahorse values were normalized by protein mass which was determined by BCA protein assay (ThermoFisher) after the measurement.

ST-*Hdh* cells were transfected with the indicated constructs (previously described (10)) with Lipofectamine 3000 as per manufacturer's protocol (Invitrogen), and treated with compounds as indicated: H_2O_2 (25 μM, 4 hours); GW501516 was at 100 nM for 24 hours. Cells were fixed with 4% PFA, and stained for TOM20 to delineate mitochondria. Cells were imaged at 63X on a Zeiss 780 confocal. Images were analyzed with the NIH Image J program using a written script from (53).

Statistical analysis

All data were prepared for analysis with standard spreadsheet software (Microsoft Excel). Statistical analysis was done using Microsoft Excel, Prism 4.0 (Graph Pad), or the VassarStats website (http://faculty.vassar.edu/lowry/VassarStats.html). For ANOVA, if statistical significance ($P < 0.05$) was achieved, we performed post-hoc analysis to account for multiple comparisons. All t-tests were two-tailed unless otherwise indicated, and the level of significance (alpha) was always set at 0.05.

Supplementary Material

Refer to Web version on PubMed Central for supplementary material.

Acknowledgments

We thank E. Lopez for technical support, and thank Y. Matsuoka for kindly providing compound GSK3787.

Funding: Supported by the Hereditary Disease Foundation, the Cure Huntington's Disease Initiative, and grants from the N.I.H. (R01 NS065874 to A.R.L., R01 AG033082 to A.R.L., and NRSA F32 NS081964 to A.S.D.). R.M.E. is an Investigator of the Howard Hughes Medical Institute at the Salk Institute and March of Dimes Chair in Molecular and Developmental Biology.

References

1. Nance MA. Genetic testing of children at risk for Huntington's disease. US Huntington Disease Genetic Testing Group. Neurology. 1997; 49:1048–1053. [PubMed: 9339688]
2. Albin RL, Reiner A, Anderson KD, Dure LSt, Handelin B, Balfour R, Whetsell WO Jr, Penney JB, Young AB. Preferential loss of striato-external pallidal projection neurons in presymptomatic Huntington's disease. Ann Neurol. 1992; 31:425–430. [PubMed: 1375014]
3. Reiner A, Albin RL, Anderson KD, D'Amato CJ, Penney JB, Young AB. Differential loss of striatal projection neurons in Huntington disease. Proceedings of the National Academy of Sciences of the United States of America. 1988; 85:5733–5737. [PubMed: 2456581]
4. Huntington's_Disease_Collaborative_Research_Group. A novel gene containing a trinucleotide repeat that is expanded and unstable on Huntington's disease chromosomes. The Huntington's Disease Collaborative Research Group. Cell. 1993; 72:971–983. [PubMed: 8458085]
5. La Spada AR, Taylor JP. Repeat expansion disease: progress and puzzles in disease pathogenesis. Nat Rev Genet. 2010; 11:247–258. [PubMed: 20177426]
6. Cui L, Jeong H, Borovecki F, Parkhurst CN, Tanese N, Krainc D. Transcriptional repression of PGC-1alpha by mutant huntingtin leads to mitochondrial dysfunction and neurodegeneration. Cell. 2006; 127:59–69. [PubMed: 17018277]
7. Lin J, Wu PH, Tarr PT, Lindenberg KS, St-Pierre J, Zhang CY, Mootha VK, Jager S, Vianna CR, Reznick RM, Cui L, Manieri M, Donovan MX, Wu Z, Cooper MP, Fan MC, Rohas LM, Zavacki AM, Cinti S, Shulman GI, Lowell BB, Krainc D, Spiegelman BM. Defects in adaptive energy metabolism with CNS-linked hyperactivity in PGC-1alpha null mice. Cell. 2004; 119:121–135. [PubMed: 15454086]
8. Weydt P, Pineda VV, Torrence AE, Libby RT, Satterfield TF, Lazarowski ER, Gilbert ML, Morton GJ, Bammler TK, Strand AD, Cui L, Beyer RP, Easley CN, Smith AC, Krainc D, Luquet S, Sweet IR, Schwartz MW, La Spada AR. Thermoregulatory and metabolic defects in Huntington's disease transgenic mice implicate PGC-1alpha in Huntington's disease neurodegeneration. Cell Metab. 2006; 4:349–362. [PubMed: 17055784]
9. Tsunemi T, Ashe TD, Morrison BE, Soriano KR, Au J, Roque RA, Lazarowski ER, Damian VA, Masliah E, La Spada AR. PGC-1alpha Rescues Huntington's Disease Proteotoxicity by Preventing Oxidative Stress and Promoting TFEB Function. Sci Transl Med. 2012; 4:142ra197.
10. Dickey AS, Pineda VV, Tsunemi T, Liu PP, Miranda HC, Gilmore-Hall SK, Lomas N, Sampat KR, Buttgereit A, Torres MJ, Flores AL, Arreola M, Arbez N, Akimov SS, Gaasterland T, Lazarowski ER, Ross CA, Yeo GW, Sopher BL, Magnuson GK, Pinkerton AB, Masliah E, La Spada AR. PPAR-delta is repressed in Huntington's disease, is required for normal neuronal function and can be targeted therapeutically. Nat Med. 2016; 22:37–45. [PubMed: 26642438]
11. Evans RM, Mangelsdorf DJ. Nuclear Receptors, RXR, and the Big Bang. Cell. 2014; 157:255–266. [PubMed: 24679540]
12. Cramer PE, Cirrito JR, Wesson DW, Lee CY, Karlo JC, Zinn AE, Casali BT, Restivo JL, Goebel WD, James MJ, Brunden KR, Wilson DA, Landreth GE. ApoE-directed therapeutics rapidly clear beta-amyloid and reverse deficits in AD mouse models. Science. 2012; 335:1503–1506. [PubMed: 22323736]
13. Mandrekar-Colucci S, Landreth GE. Nuclear receptors as therapeutic targets for Alzheimer's disease. Expert Opin Ther Targets. 2011; 15:1085–1097. [PubMed: 21718217]

14. Girroir EE, Hollingshead HE, He P, Zhu B, Perdew GH, Peters JM. Quantitative expression patterns of peroxisome proliferator-activated receptor-beta/delta (PPARbeta/delta) protein in mice. Biochem Biophys Res Commun. 2008; 371:456–461. [PubMed: 18442472]
15. Malm T, Mariani M, Donovan LJ, Neilson L, Landreth GE. Activation of the nuclear receptor PPARdelta is neuroprotective in a transgenic mouse model of Alzheimer's disease through inhibition of inflammation. J Neuroinflammation. 2015; 12:7. [PubMed: 25592770]
16. Schilling G, Becher MW, Sharp AH, Jinnah HA, Duan K, Kotzuk JA, Slunt HH, Ratovitski T, Cooper JK, Jenkins NA, Copeland NG, Price DL, Ross CA, Borchelt DR. Intranuclear inclusions and neuritic aggregates in transgenic mice expressing a mutant N-terminal fragment of huntingtin. Hum Mol Genet. 1999; 8:397–407. [PubMed: 9949199]
17. Tesseur I, Lo AC, Roberfroid A, Dietvorst S, Van Broeck B, Borgers M, Gijsen H, Moechars D, Mercken M, Kemp J, D'Hooge R, De Strooper B. Comment on “ApoE-directed therapeutics rapidly clear beta-amyloid and reverse deficits in AD mouse models”. Science. 2013; 340:924-e.
18. Wang S, Wen P, Wood S. Effect of LXR/RXR agonism on brain and CSF Abeta40 levels in rats. F1000Res. 2016; 5:138. [PubMed: 27239272]
19. Landis SC, Amara SG, Asadullah K, Austin CP, Blumenstein R, Bradley EW, Crystal RG, Darnell RB, Ferrante RJ, Fillit H, Finkelstein R, Fisher M, Gendelman HE, Golub RM, Goudreau JL, Gross RA, Gubitz AK, Hesterlee SE, Howells DW, Huguenard J, Kelner K, Koroshetz W, Krainc D, Lazic SE, Levine MS, Macleod MR, McCall JM, Moxley RT 3rd, Narasimhan K, Noble LJ, Perrin S, Porter JD, Steward O, Unger E, Utz U, Silberberg SD. A call for transparent reporting to optimize the predictive value of preclinical research. Nature. 2012; 490:187–191. [PubMed: 23060188]
20. Perrin S. Preclinical research: Make mouse studies work. Nature. 2014; 507:423–425. [PubMed: 24678540]
21. Guyenet SJ, Furrer SA, Damian VM, Baughan TD, La Spada AR, Garden GA. A simple composite phenotype scoring system for evaluating mouse models of cerebellar ataxia. J Vis Exp. 2010
22. Luquet S, Lopez-Soriano J, Holst D, Fredenrich A, Melki J, Rassoulzadegan M, Grimaldi PA. Peroxisome proliferator-activated receptor delta controls muscle development and oxidative capability. Faseb J. 2003; 17:2299–2301. [PubMed: 14525942]
23. Schuler M, Ali F, Chambon C, Duteil D, Bornert JM, Tardivel A, Desvergne B, Wahli W, Chambon P, Metzger D. PGC1alpha expression is controlled in skeletal muscles by PPARbeta, whose ablation results in fiber-type switching, obesity, and type 2 diabetes. Cell Metab. 2006; 4:407–414. [PubMed: 17084713]
24. Lin MT, Beal MF. Mitochondrial dysfunction and oxidative stress in neurodegenerative diseases. Nature. 2006; 443:787–795. [PubMed: 17051205]
25. Caro P, Kishan AU, Norberg E, Stanley IA, Chapuy B, Ficarro SB, Polak K, Tondera D, Gounarides J, Yin H, Zhou F, Green MR, Chen L, Monti S, Marto JA, Shipp MA, Danial NN. Metabolic signatures uncover distinct targets in molecular subsets of diffuse large B cell lymphoma. Cancer Cell. 2012; 22:547–560. [PubMed: 23079663]
26. Labbadia J, Morimoto RI. The biology of proteostasis in aging and disease. Annu Rev Biochem. 2015; 84:435–464. [PubMed: 25784053]
27. Trettel F, Rigamonti D, Hilditch-Maguire P, Wheeler VC, Sharp AH, Persichetti F, Cattaneo E, MacDonald ME. Dominant phenotypes produced by the HD mutation in STHdh(Q111) striatal cells. Hum Mol Genet. 2000; 9:2799–2809. [PubMed: 11092756]
28. Frank M, Duvezin-Caubet S, Koob S, Occhipinti A, Jagasia R, Petcherski A, Ruonala MO, Priault M, Salin B, Reichert AS. Mitophagy is triggered by mild oxidative stress in a mitochondrial fission dependent manner. Biochim Biophys Acta. 2012; 1823:2297–2310. [PubMed: 22917578]
29. Settembre C, Di Malta C, Polito VA, Garcia Arencibia M, Vetrini F, Erdin S, Erdin SU, Huynh T, Medina D, Colella P, Sardiello M, Rubinsztein DC, Ballabio A. TFEB links autophagy to lysosomal biogenesis. Science. 2011; 332:1429–1433. [PubMed: 21617040]
30. Chaturvedi RK, Adhihetty P, Shukla S, Hennessy T, Calingasan N, Yang L, Starkov A, Kiaei M, Cannella M, Sassone J, Ciammola A, Squitieri F, Beal MF. Impaired PGC-1alpha function in muscle in Huntington's disease. Hum Mol Genet. 2009; 18:3048–3065. [PubMed: 19460884]

31. Fitz NF, Cronican AA, Lefterov I, Koldamova R. Comment on “ApoE-directed therapeutics rapidly clear beta-amyloid and reverse deficits in AD mouse models”. Science. 2013; 340:924-c.
32. Ghosal K, Haa M, Verghese PB, West T, Veenstra T, Braunstein JB, Bateman RJ, Holtzman DM, Landreth GE. A randomized controlled study to evaluate the effect of bexarotene on amyloid-β and apolipoprotein E metabolism in healthy subjects - Alzheimer's & Dementia: Translational Research & Clinical Interventions. Alzheimer's & Dementia: Translational Research & Clinical Interventions. 2016; 2:110–120.
33. Kuntz M, Candela P, Saint-Pol J, Lamartiniere Y, Boucau MC, Sevin E, Fenart L, Gosselet F. Bexarotene Promotes Cholesterol Efflux and Restricts Apical-to-Basolateral Transport of Amyloid-beta Peptides in an In Vitro Model of the Human Blood-Brain Barrier. J Alzheimers Dis. 2015; 48:849–862. [PubMed: 26402114]
34. Fan W, Waizenegger W, Lin CS, Sorrentino V, He MX, Wall CE, Li H, Liddle C, Yu RT, Atkins AR, Auwerx J, Downes M, Evans RM. PPARdelta Promotes Running Endurance by Preserving Glucose. Cell Metab. 2017; 25:1186–1193. e1184. [PubMed: 28467934]
35. Koh JH, Hancock CR, Terada S, Higashida K, Holloszy JO, Han DH. PPARbeta Is Essential for Maintaining Normal Levels of PGC-1alpha and Mitochondria and for the Increase in Muscle Mitochondria Induced by Exercise. Cell Metab. 2017; 25:1176–1185. e1175. [PubMed: 28467933]
36. Weydt P, La Spada AR. Targeting protein aggregation in neurodegeneration--lessons from polyglutamine disorders. Expert Opin Ther Targets. 2006; 10:505–513. [PubMed: 16848688]
37. Shirendeb UP, Calkins MJ, Manczak M, Anekonda V, Dufour B, McBride JL, Mao P, Reddy PH. Mutant huntingtin's interaction with mitochondrial protein Drp1 impairs mitochondrial biogenesis and causes defective axonal transport and synaptic degeneration in Huntington's disease. Hum Mol Genet. 2012; 21:406–420. [PubMed: 21997870]
38. Song W, Chen J, Petrilli A, Liot G, Klinglmayr E, Zhou Y, Poquiz P, Tjong J, Pouladi MA, Hayden MR, Masliah E, Ellisman M, Rouiller I, Schwarzenbacher R, Bossy B, Perkins G, Bossy-Wetzel E. Mutant huntingtin binds the mitochondrial fission GTPase dynamin-related protein-1 and increases its enzymatic activity. Nat Med. 2011; 17:377–382. [PubMed: 21336284]
39. Tellez-Nagel I, Johnson AB, Terry RD. Studies on brain biopsies of patients with Huntington's chorea. J Neuropathol Exp Neurol. 1974; 33:308–332. [PubMed: 4150800]
40. Cherubini M, Puigdellivol M, Alberch J, Gines S. Cdk5-mediated mitochondrial fission: A key player in dopaminergic toxicity in Huntington's disease. Biochim Biophys Acta. 2015; 1852:2145–2160. [PubMed: 26143143]
41. Haun F, Nakamura T, Shiu AD, Cho DH, Tsunemi T, Holland EA, La Spada AR, Lipton SA. S-nitrosylation of dynamin-related protein 1 mediates mutant huntingtin-induced mitochondrial fragmentation and neuronal injury in Huntington's disease. Antioxid Redox Signal. 2013; 19:1173–1184. [PubMed: 23641925]
42. Palomer X, Capdevila-Busquets E, Botteri G, Salvado L, Barroso E, Davidson MM, Michalik L, Wahli W, Vazquez-Carrera M. PPARbeta/delta attenuates palmitate-induced endoplasmic reticulum stress and induces autophagic markers in human cardiac cells. Int J Cardiol. 2014; 174:110–118. [PubMed: 24767130]
43. Guedes-Dias P, de Proenca J, Soares TR, Leitao-Rocha A, Pinho BR, Duchen MR, Oliveira JM. HDAC6 inhibition induces mitochondrial fusion, autophagic flux and reduces diffuse mutant huntingtin in striatal neurons. Biochim Biophys Acta. 2015; 1852:2484–2493. [PubMed: 26300485]
44. Vakeva L, Ranki A, Hahtola S. Ten-year experience of bexarotene therapy for cutaneous T-cell lymphoma in Finland. Acta Derm Venereol. 2012; 92:258–263. [PubMed: 22678563]
45. Gines S, Seong IS, Fossale E, Ivanova E, Trettel F, Gusella JF, Wheeler VC, Persichetti F, MacDonald ME. Specific progressive cAMP reduction implicates energy deficit in presymptomatic Huntington's disease knock-in mice. Hum Mol Genet. 2003; 12:497–508. [PubMed: 12588797]
46. Young JE, Martinez RA, La Spada AR. Nutrient deprivation induces neuronal autophagy and implicates reduced insulin signaling in neuroprotective autophagy activation. The Journal of biological chemistry. 2009; 284:2363–2373. [PubMed: 19017649]

47. Young JE, Garden GA, Martinez RA, Tanaka F, Sandoval CM, Smith AC, Sopher BL, Lin A, Fischbeck KH, Ellerby LM, Morrison RS, Taylor JP, La Spada AR. Polyglutamine-expanded androgen receptor truncation fragments activate a Bax-dependent apoptotic cascade mediated by DP5/Hrk. J Neurosci. 2009; 29:1987–1997. [PubMed: 19228953]

48. Watkin EE, Arbez N, Waldron-Roby E, O'Meally R, Ratovitski T, Cole RN, Ross CA. Phosphorylation of mutant huntingtin at serine 116 modulates neuronal toxicity. PLoS One. 2014; 9:e88284. [PubMed: 24505464]

49. Kaltenbach LS, Bolton MM, Shah B, Kanju PM, Lewis GM, Turmel GJ, Whaley JC, Trask OJ Jr, Lo DC. Composite primary neuronal high-content screening assay for Huntington's disease incorporating non-cell-autonomous interactions. J Biomol Screen. 2010; 15:806–819. [PubMed: 20581077]

50. Guyenet SJ, Furrer SA, Damian VM, Baughan TD, La Spada AR, Garden GA. A simple composite phenotype scoring system for evaluating mouse models of cerebellar ataxia. J Vis Exp. 2010

51. Livak KJ, Flood SJ, Marmaro J, Giusti W, Deetz K. Oligonucleotides with fluorescent dyes at opposite ends provide a quenched probe system useful for detecting PCR product and nucleic acid hybridization. PCR Methods Appl. 1995; 4:357–362. [PubMed: 7580930]

52. Bustin SA. Quantification of mRNA using real-time reverse transcription PCR (RT-PCR): trends and problems. J Mol Endocrinol. 2002; 29:23–39. [PubMed: 12200227]

53. Dickey AS, Strack S. PKA/AKAP1 and PP2A/Bbeta2 regulate neuronal morphogenesis via Drp1 phosphorylation and mitochondrial bioenergetics. J Neurosci. 2011; 31:15716–15726. [PubMed: 22049414]

Accessible Summary

PPARδ is a permissive nuclear receptor that heterodimerizes with RXR to activate target genes. Interference with transcription of the *PPARδ* gene contributes to neurodegeneration in Huntington's disease (HD). In new work, Dickey et al. evaluated the RXR agonist bexarotene in cellular models of HD and in a mouse model in vivo. They determined that bexarotene was effective at countering HD neurotoxicity in mouse primary neurons and in human HD patient stem cell-derived neurons, and in the BAC-HD mouse model. The authors then examined the basis for PPARδ neuroprotection and found that RXR/PPARδ agonist therapy enhanced oxidative metabolism, promoted mitochondrial quality control, and boosted protein homeostasis by activating autophagy.

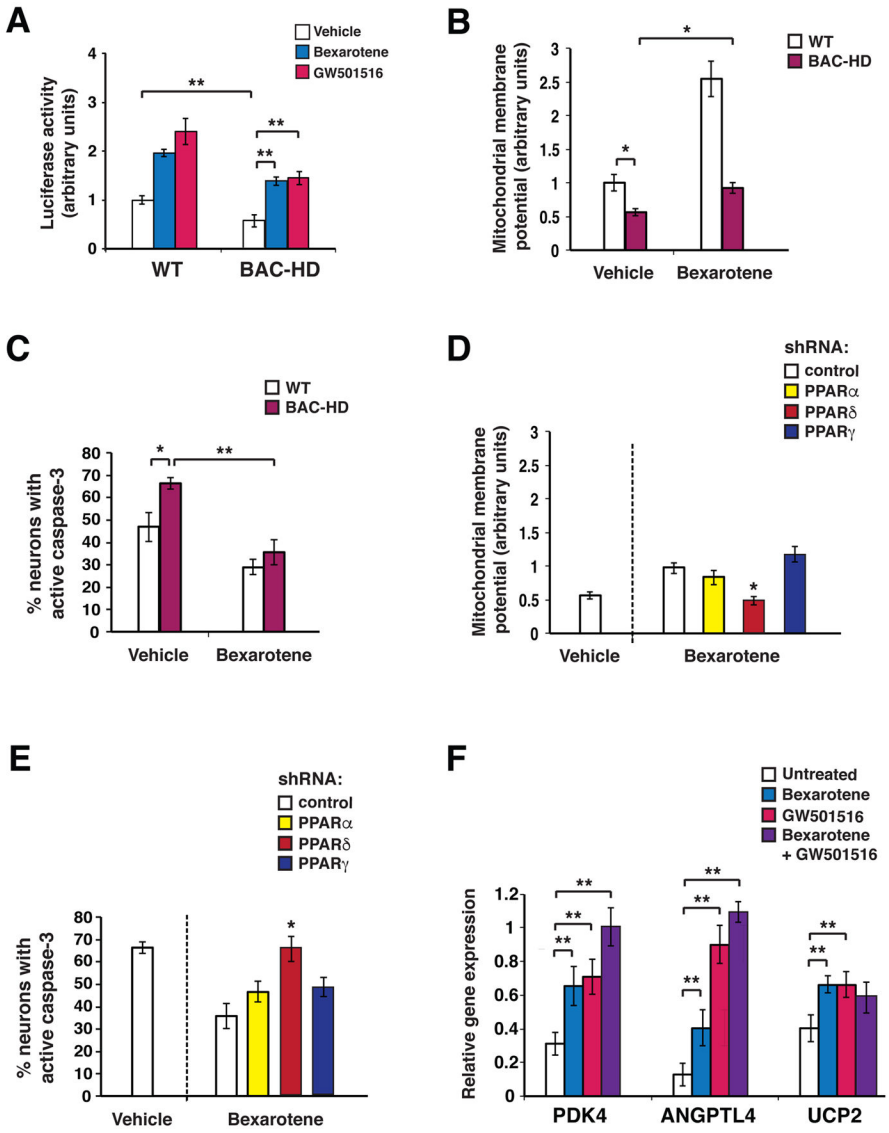

Figure 1. Bexarotene promotes PPARδ activation to ameliorate the neurotoxicity of mutant huntingtin

(A) We measured 3X-PPRE luciferase reporter activity in primary cortical neurons from wild-type (WT) control mice or BAC-HD mice, co-transfected with Renilla luciferase vector, and treated with bexarotene (500 nM), GW501516 (100 nM), or vehicle. PPARδ activation in BAC-HD mouse neurons was repressed at baseline compared to WT mouse neurons. $^{**}P < 0.01$, Student's t-test. Bexarotene and GW501516 treatment promoted PPARδ activation in BAC-HD mouse neurons. $^{**}P < 0.01$, ANOVA with post-hoc Tukey test. n = 3 biological replicates; n = 3 technical replicates. Results were normalized to WT mouse neurons at baseline. (B) Mitochondrial membrane potential of primary cortical neurons from WT and BAC-HD mice, treated with vehicle or bexarotene (500 nM), was determined from the ratio of mitochondrial to cytosolic JC-1 fluorescence. $^{*}P < 0.05$, Student's t-test. n = 3 biological replicates; n = 3 technical replicates. Results were normalized to WT mouse neurons at baseline. Similar results were obtained using TMRM as

the fluorescent probe (Fig. S1B). (C) We quantified active caspase-3 immunostaining of primary cortical neurons from WT and BAC-HD mice, treated with vehicle or bexarotene (500 nM) for 24 hours, and H_2O_2 (25 μM for 4 hours). *$P < 0.05$, **$P < 0.01$; Student's t-test. n = 3 biological replicates; 30 to 50 cells were counted/experiment. (D) Mitochondrial membrane potential was measured in BAC-HD mouse primary cortical neurons, transfected with the indicated shRNA expression vector (control = scrambled shRNA), and treated with vehicle or bexarotene (500 nM). Mitochondrial membrane potential was determined from the ratio of mitochondrial to cytosolic JC-1 fluorescence. *$P < 0.05$; ANOVA with post-hoc Tukey test. n = 3 biological replicates; n = 3 technical replicates. Results were normalized to WT mouse neurons at baseline as in panel B. (E) We quantified active caspase-3 immunostaining of BAC-HD mouse primary cortical neurons, transfected with the indicated shRNA expression vectors, and treated with vehicle or bexarotene (500 nM) for 24 hours, and H_2O_2 (25 μM, for 4 hours). *$P < 0.05$; ANOVA with post-hoc Tukey test. n = 3 biological replicates; 30 to 50 cells were counted/experiment. (F) We performed RT-PCR analysis of RNA expression of the PPARδ target genes PDK4, Angptl4, and UCP2 in BAC-HD mouse primary cortical neurons, treated as indicated. **$P < 0.01$; ANOVA with post-hoc Tukey test. n = 6 independent experiments. Error bars = s.e.m.

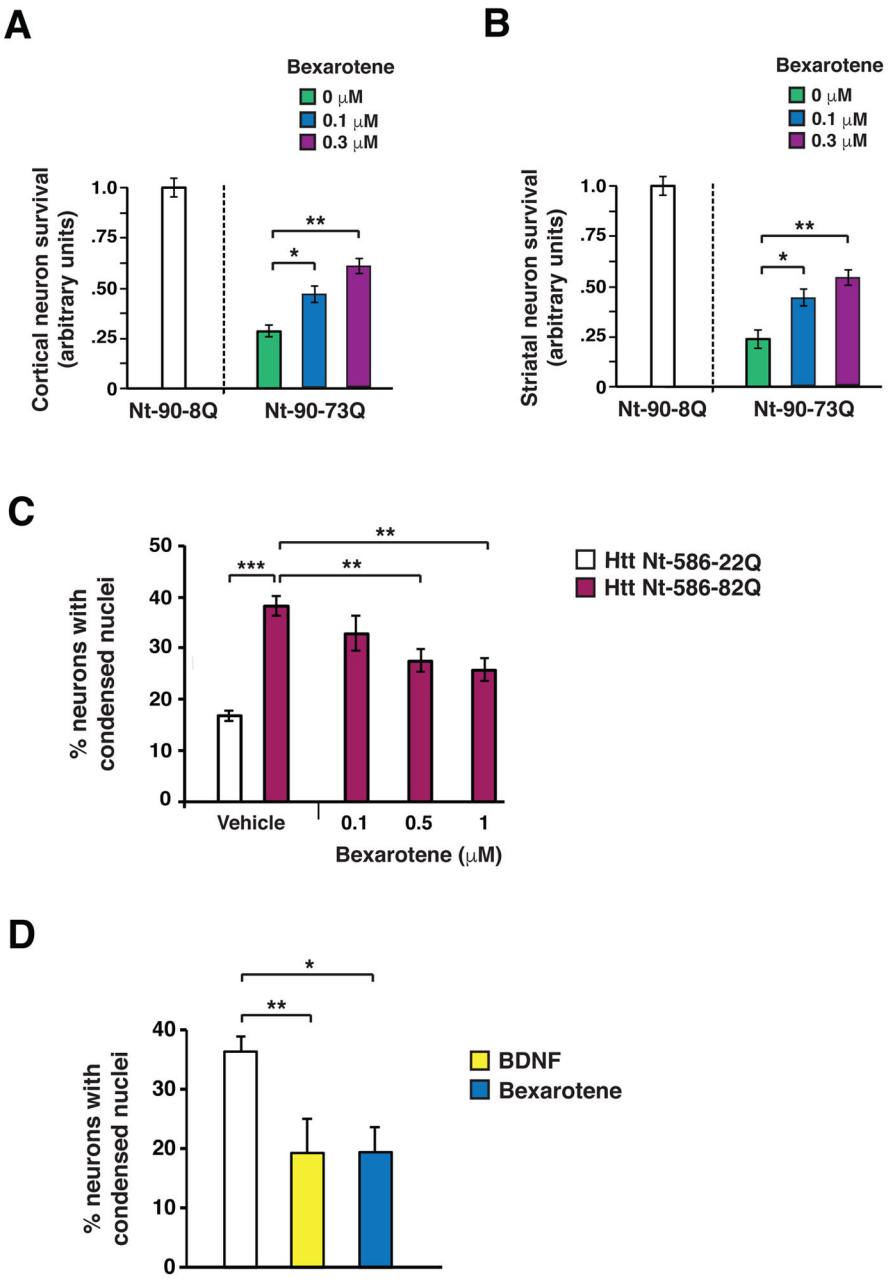

Figure 2. Bexarotene is neuroprotective in mouse and human HD neurons in vitro

(A) We measured survival of cortical neurons in mouse CD1 strain cortical neuron-striatal neuron co-cultures transfected with the indicated Htt expression vector, and treated with bexarotene at the indicated concentration. Total numbers counted for fluorescently transfected neurons for each condition were normalized to Htt Nt-90-8Q-transfected neurons at baseline, with neuron survival arbitrarily set to 1. $*P < 0.05$, $**P < 0.01$; Student's t-test. n = 3 independent experiments. (B) We measured survival of striatal neurons in cortical neuron-striatal neuron co-cultures transfected with the indicated Htt expression vector, and treated with bexarotene at the indicated concentration. Total numbers counted for fluorescently transfected neurons for each condition were normalized to Htt Nt-90-8Q-

transfected neurons at baseline, with survival arbitrarily set to 1. *$P < 0.05$, **$P < 0.01$, Student's t-test. n = 3 independent experiments. (C) We quantified cell death in mouse primary cortical neurons, transfected with the indicated Htt expression vector, and treated with vehicle or bexarotene at the indicated concentration. **$P < 0.01$, ***$P < 0.001$; Student's t-test. n = 6 independent experiments. (D)We quantified cell death in medium spiny-like neurons differentiated from an induced pluripotent stem cell line derived from a patient with HD carrying a 60Q allele in the huntingtin gene, and treated with bexarotene (1.0 μM) or BDNF (20 ng/ml). *$P < 0.05$, **$P < 0.01$; Student's t-test. n = 3 independent experiments. Error bars = s.e.m.

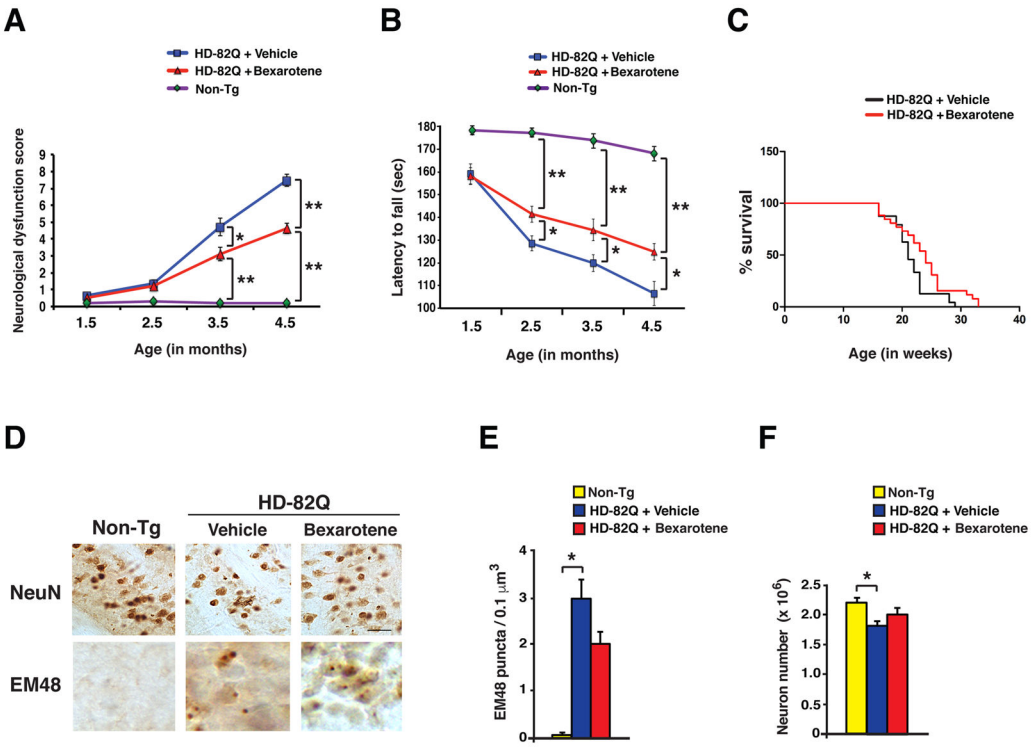

Figure 3. Bexarotene is neuroprotective in the N171-82Q mouse model of HD

(A) We recorded neurological dysfunction scores (0 – 12, where 0 = normal and 12 = severely affected) in cohorts (n = 10 – 19 mice / group) of non-transgenic control mice (Non-Tg), vehicle-treated HD mice, and bexarotene-treated HD mice at monthly intervals, beginning at the initiation of the treatment. *$P < 0.05$, **$P < 0.01$; ANOVA with post-hoc Tukey test. (B) We measured times for the latency to fall on the rotarod test in cohorts (n = 12 – 24 mice / group) of non-transgenic control mice (Non-Tg), vehicle-treated HD mice, and bexarotene-treated HD mice at monthly intervals, beginning at the initiation of the treatment. *$P < 0.05$, **$P < 0.01$; ANOVA with post-hoc Tukey test. (C) We measured survival of vehicle-treated HD mice (n = 24) and bexarotene-treated HD mice (n = 26) over time. Bexarotene-treated HD mice lived longer than did vehicle-treated HD mice. $P < 0.05$; Log-rank test. (D) Sections of striatum from 18 week-old non-transgenic control mice (Non-Tg), vehicle-treated HD mice, and bexarotene-treated HD mice (n = 5 – 7 mice / group) were immunostained for the neuronal marker NeuN and anti-polyglutamine antibody EM48. Scale bar = 20 μm. (E) We quantified EM48 puncta from the data in panel D. *$P < 0.05$; ANOVA with post-hoc Tukey test. n = 5 – 8 mice / group. (F) We quantified neuron numbers from data in panel D. *$P < 0.05$; ANOVA with post-hoc Tukey test. n = 5 – 8 mice/group. Error bars = s.e.m.

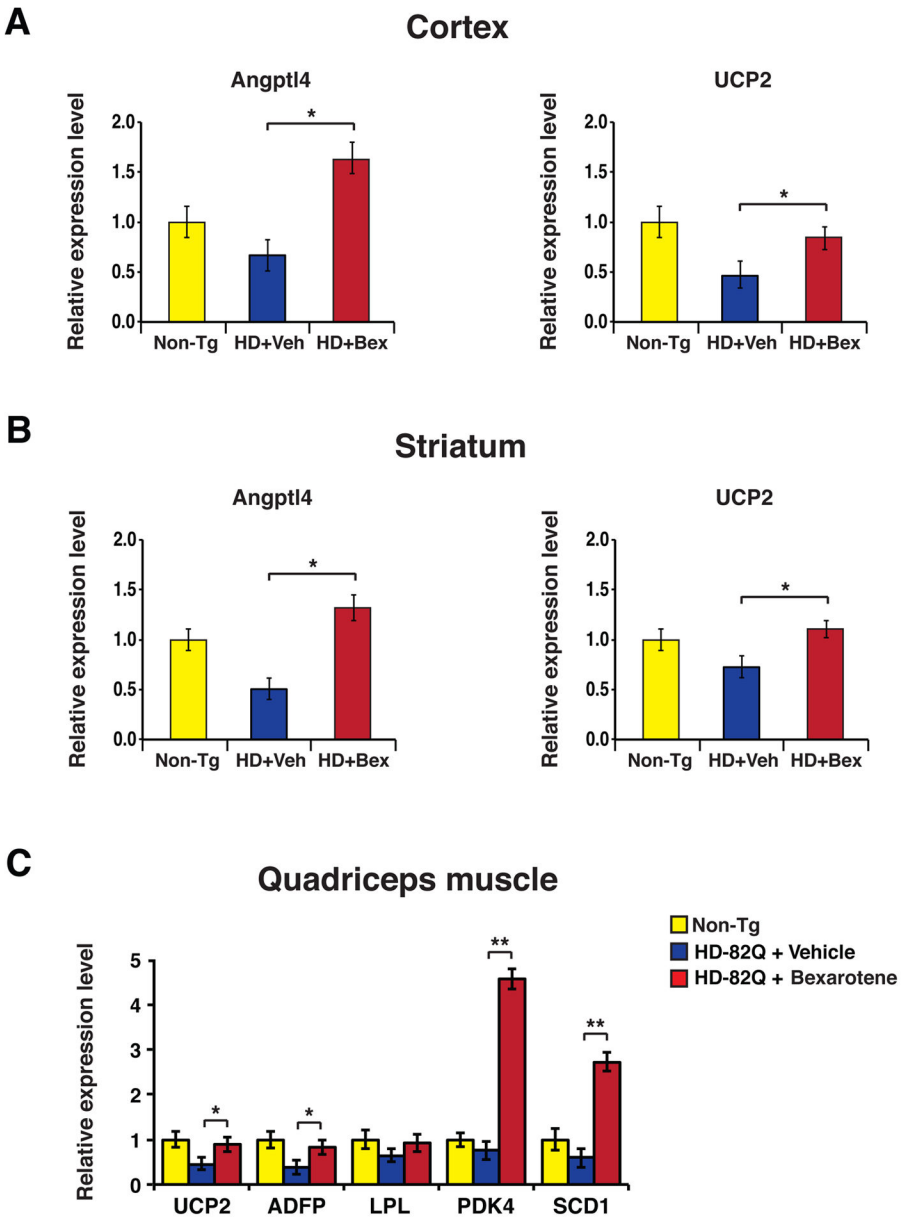

Figure 4. Bexarotene promotes PPARδ activation of target genes in mouse brain and muscle

(A) We performed RT-PCR analysis to measure RNA expression of the PPARδ target genes Angptl4 and UCP2 in the cortex of 18 week-old non-transgenic control mice (Non-Tg), vehicle-treated HD mice, and bexarotene-treated HD mice. $^{**}P < 0.01$; ANOVA with post-hoc Tukey test. n = 9 – 12 mice / group. (B) We performed RT-PCR analysis of RNA expression of Angptl4 and UCP2 in the striatum of 18 week-old non-transgenic control mice (Non-Tg), vehicle-treated HD mice, and bexarotene-treated HD mice. $^{**}P < 0.01$; ANOVA with post-hoc Tukey test. n = 9 – 12 mice / group. (C) We performed RT-PCR analysis of RNA expression of five PPARδ target genes in the quadriceps muscle of 18 week-old non-transgenic control mice (Non-Tg), vehicle-treated HD mice, and bexarotene-treated HD

mice. *$P < 0.05$, **$P < 0.01$; ANOVA with post-hoc Tukey test. n = 9 mice / group. Error bars = s.e.m.

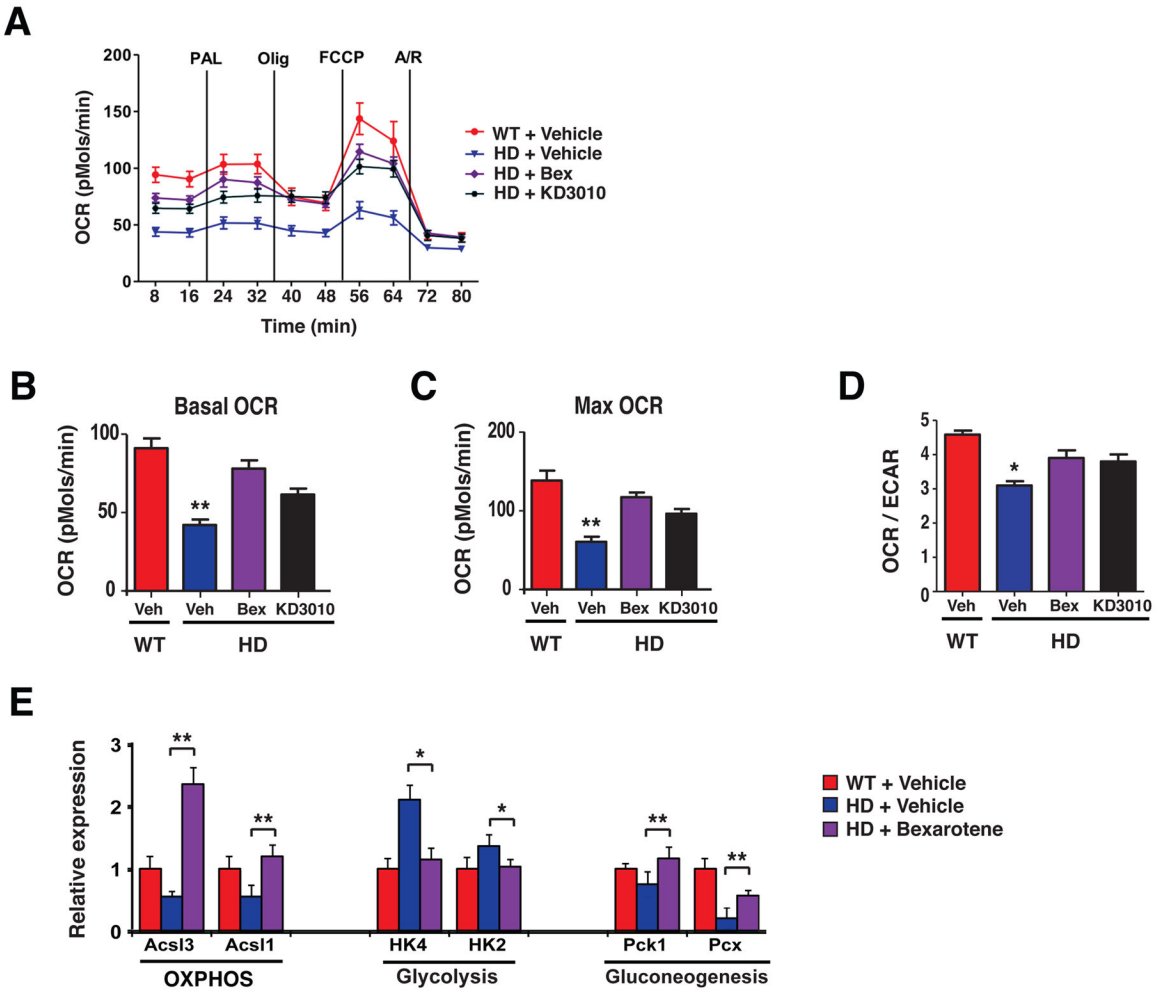

Figure 5. PPARδ agonist treatment reverses impaired oxidative metabolism in mouse HD neurons

(A) Mitochondrial respiratory states were assessed by extracellular flux analysis in primary cortical neurons obtained from BAC-HD mice (HD) and littermate controls (WT), and treated with vehicle (Veh), bexarotene (500 nM, Bex), or KD3010 (100 nM). (B) We quantified basal oxygen consumption rate (OCR) in neurons from panel A. $^{**}P < 0.01$; ANOVA with post-hoc Tukey test. n = 6 – 7 samples / condition. (C) We quantified maximal OCR in neurons from panel A. $^{**}P < 0.01$; ANOVA with post-hoc Tukey test. n = 6 – 7 samples / condition. (D) We calculated OCR / extracellular acidification rate (ECAR) in neurons from panel B. $^{*}P < 0.05$; ANOVA with post-hoc Tukey test. n = 6 – 7 samples / condition. (E) We performed RT-PCR analysis of RNA expression of the PPARδ target genes *Ascl1, Ascl3, Hk2, Hk4, Pck* and *Pcx* (representative of different metabolic pathways) in the striatum of 18 week-old vehicle-treated non-transgenic control mice (WT), vehicle-treated HD mice, and bexarotene-treated HD mice. $^{*}P < 0.05$, $^{**}P < 0.01$; ANOVA with post-hoc Tukey test. n = 3 mice / group. Error bars = s.e.m.

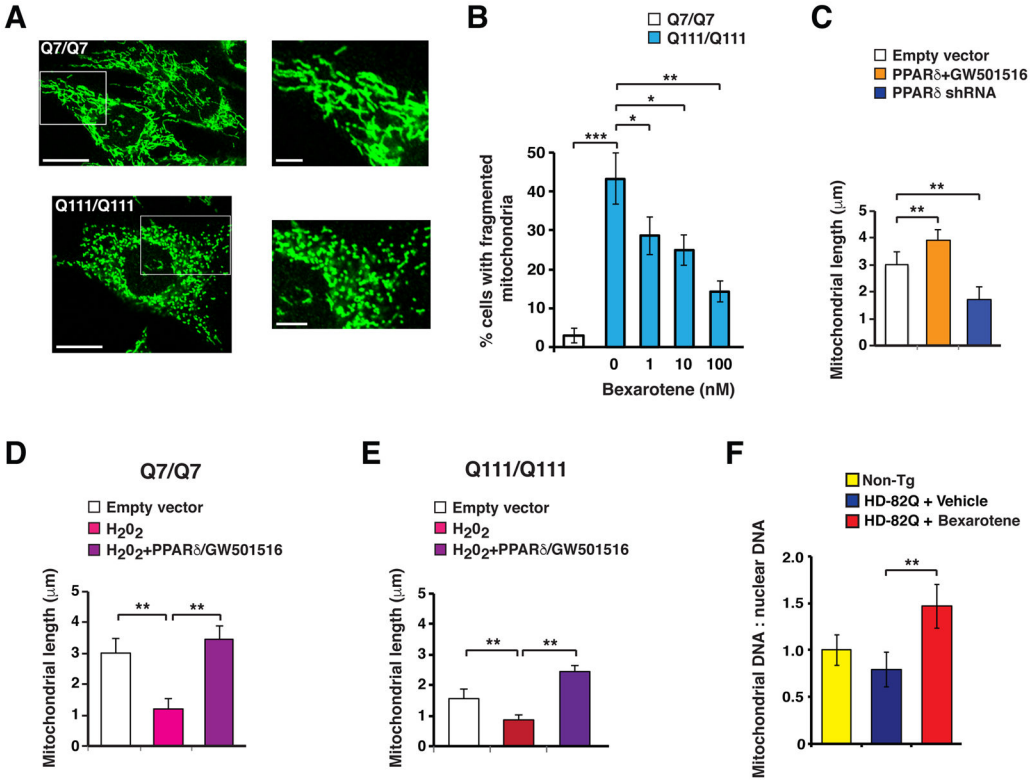

Figure 6. Bexarotene activation of PPARδ rescues altered mitochondrial morphology and protein quality control in HD mouse neurons

(A) Shown are representative images of striatal-like cells from ST-*Hdh* Q7/Q7 (control) and ST-*Hdh* Q111/Q111 (HD) knock-in mice immunostained with Tom20 antibody. Note tubular appearance of mitochondrial network in the Q7/Q7 cells, compared to fragmented appearance of mitochondrial network in the Q111/Q111 cells. Scale bars, 20 μm and 5 μm (inset). (B) We classified the mitochondrial network of ST-*Hdh* cells as tubular or fragmented as in (A), and then determined the % cells with fragmented mitochondria. Approximately 43% of Q111/Q111 cells contained a fragmented mitochondrial network, whereas only ~3% of Q7/Q7 cells contained a fragmented mitochondrial network. ** P<0.01; Student's t-test. Treatment of Q111/Q111 cells with bexarotene reduced mitochondrial fragmentation in a dose-dependent manner. * P<0.05, ** P < 0.01; ANOVA with post-hoc Tukey test. n = 51 – 87 cells / plate, 6 – 9 plates / cell line. (C) We measured average mitochondrial length in ST-*Hdh* Q7/Q7 striatal-like cells immunostained with Tom20 antibody as in (A), and transfected with a PPARδ expression vector and treated with GW501516, or transfected with a PPARδ shRNA expression construct, as indicated. ** P < 0.01; ANOVA with post-hoc Tukey test. n = 42 – 56 cells / plate, 3 plates / condition. (D) We measured average mitochondrial length in ST-*Hdh* Q7/Q7 striatal-like cells immunostained with Tom20 antibody as in (A), and treated with hydrogen peroxide with or without PPARδ expression vector transfection and GW501516 treatment, as indicated. ** P < 0.01; ANOVA with post-hoc Tukey test. n = 38 – 56 cells / plate, 3 plates / condition. (E) We measured average mitochondrial length in ST-*Hdh* Q111/Q111 striatal-like cells immunostained with Tom20 antibody as in (A), and treated with hydrogen peroxide with or without PPARδ expression vector transfection and GW501516 treatment, as indicated. ** P

< 0.01; ANOVA with post-hoc Tukey test. n = 35 – 47 cells / plate, 3 plates / condition. (F) We performed qPCR analysis of a mitochondrial genomic amplicon and a nuclear genomic amplicon, and determined the ratio of mitochondrial DNA to nuclear DNA in the striatum of 18 week-old non-transgenic control mice (Non-Tg), vehicle-treated HD mice, and bexarotene-treated HD mice. $^{**}P < 0.01$; ANOVA with post-hoc Tukey test. n = 9 – 12 mice / group. Error bars = s.e.m.

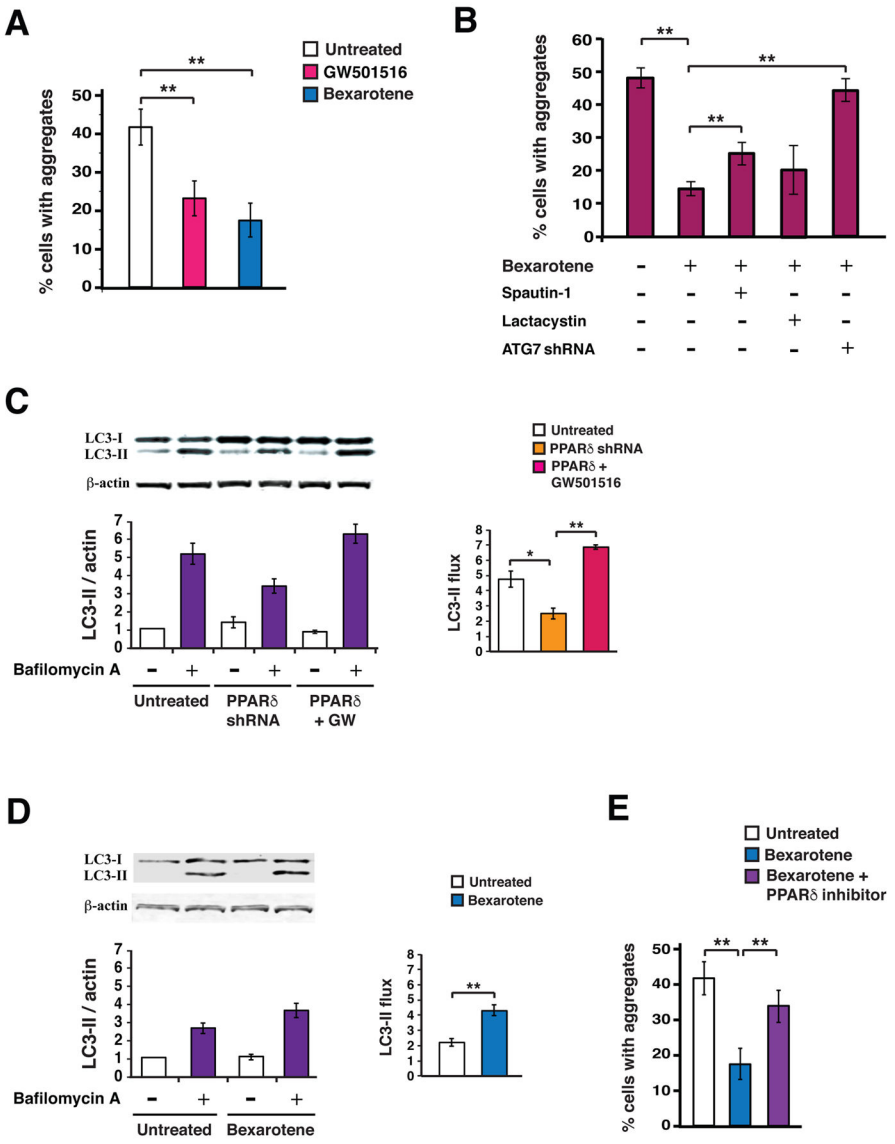

Figure 7. Bexarotene activation of PPARδ promotes proteostasis by inducing the autophagy pathway in mouse neurons

(A) We quantified the percentage of Neuro2a cells containing htt protein aggregates, when transfected with a htt-104Q expression vector, treated for 24 hours with GW501516 (500 nM) or Bexarotene (1 μM), and exposed to H_2O_2 (25μM for 4 hours). $^{**}P < 0.01$; ANOVA with post-hoc Tukey test. n = 30 – 50 cells / sample, 9 samples / condition. (B) We quantified the percentage of Neuro2a cells containing htt protein aggregates, when transfected with a htt-104Q expression vector, treated for 24 hours with Bexarotene (1 μM), Spautin-1 (10 nM) or Lactacystin (5 nM), and exposed to H_2O_2 (25μM for 4 hours). $^{**}P < 0.01$; ANOVA with post-hoc Tukey test. n = 30 – 50 cells / sample, 9 – 12 samples / condition. (C) We performed microtubule-associated protein 1A/1B-light chain 3 (LC3) immunoblot analysis of Neuro2a cells cultured in normal media in the presence or absence of bafilomycin, and transfected with a PPARδ shRNA vector, or a PPARδ expression vector and treated with GW501516 (100 nM). β-actin served as a loading control. (D) We

performed densitometry analysis of the LC3 immunoblotting results shown in (C) to determine autophagy flux. *P<0.05, **P < 0.01; ANOVA with post-hoc Tukey test. n = 3 independent experiments. (E) We quantified the percentage of Neuro2a cells containing htt protein aggregates, when transfected with a htt-104Q expression vector, treated with bexarotene (500 nM) alone, or bexarotene (500 nM) plus the PPARδ inhibitor GSK3787 (200 nM), and exposed to H_2O_2 (25μM for 4 hours). **P < 0.01; ANOVA with post-hoc Tukey test. n = 30 – 50 cells / sample, 9 samples / condition. Error bars = s.e.m.